Essential but differential role for CXCR4 and CXCR7 in the therapeutic homing of human renal progenitor cells

Benedetta Mazzinghi,[1] Elisa Ronconi,[1] Elena Lazzeri,[1] Costanza Sagrinati,[1] Lara Ballerini,[1] Maria Lucia Angelotti,[1] Eliana Parente,[1] Rosa Mancina,[1] Giuseppe Stefano Netti,[3] Francesca Becherucci,[1] Mauro Gacci,[2] Marco Carini,[2] Loreto Gesualdo,[3] Mario Rotondi,[1,4] Enrico Maggi,[1] Laura Lasagni,[1] Mario Serio,[1] Sergio Romagnani,[1] and Paola Romagnani[1]

[1]Excellence Center for Research, Transfer and High Education DENOthe, and [2]Department of Medical and Surgical Critical Care, University of Florence, 50121 Florence, Italy
[3]Department of Biomedical Sciences, University of Foggia, 71100 Foggia, Italy
[4]Department of Endocrinology and Internal Medicine, Fondazione Salvatore Maugeri Istituto Di Ricovero e Cura a Carattere Scientifico, 27100 Pavia, Italy

Recently, we have identified a population of renal progenitor cells in human kidneys showing regenerative potential for injured renal tissue of SCID mice. We demonstrate here that among all known chemokine receptors, human renal progenitor cells exhibit high expression of both stromal-derived factor-1 (SDF-1) receptors, CXCR4 and CXCR7. In SCID mice with acute renal failure (ARF), SDF-1 was strongly up-regulated in resident cells surrounding necrotic areas. In the same mice, intravenously injected renal stem/progenitor cells engrafted into injured renal tissue decreased the severity of ARF and prevented renal fibrosis. These beneficial effects were abolished by blocking either CXCR4 or CXCR7, which dramatically reduced the number of engrafting renal progenitor cells. However, although SDF-1–induced migration of renal progenitor cells was only abolished by an anti-CXCR4 antibody, transendothelial migration required the activity of both CXCR4 and CXCR7, with CXCR7 being essential for renal progenitor cell adhesion to endothelial cells. Moreover, CXCR7 but not CXCR4 was responsible for the SDF-1–induced renal progenitor cell survival. Collectively, these findings suggest that CXCR4 and CXCR7 play an essential, but differential, role in the therapeutic homing of human renal progenitor cells in ARF, with important implications for the development of stem cell–based therapies.

CORRESPONDENCE
Paola Romagnani:
p.romagnani@dfc.unifi.it

Abbreviations used: ARF, acute renal failure; BMSC, BM-derived SC; BUN, blood urea nitrogen; EBM, endothelial basal medium; EC, endothelial cell; HSC, hematopoietic SC; HUVEC, human umbilical vein EC; I-TAC, interferon-induced T cell α chemoattractant; LTA, Lotus tetragonolobus agglutinin; RMP, renal multipotent progenitor; RPTEC, renal proximal tubular cell; SC, stem cell; SDF, stromal-derived factor.

Adult stem cells (SCs) have been described to contribute to tissue regeneration after injury in various organ systems (1). The recruitment of SCs to the injured tissue herein appears to be the prerequisite for SC-based repair, and the comprehension of mechanisms that regulate their migration is crucial for the success of any clinical strategy involving SCs (2). In this context, the chemokine stromal-derived factor-1 (SDF-1) has been implicated as a principal regulator of retention, migration, and mobilization of hematopoietic SCs (HSCs) and endothelial progenitor cells during steady-state homeostasis and injury (2). In addition, SDF-1 is considered as a critical mediator of recruitment and transendothelial migration in successful therapeutic strategies that involve the ex vivo injection of resident tissue SCs (1–4). CXCR4 has long been considered as the unique receptor of SDF-1 and as the only mediator of SDF-1-induced biological effects (5–6). Recently, however, SDF-1 was reported to also be a ligand of a novel chemokine receptor, CXCR7 (7). In human tissues, CXCR7 expression has been described on endothelial cells (ECs) and on some tumor cell lines, but its contribution to SDF-1–mediated effects is still unknown.

Acute renal failure (ARF) is a leading cause of morbidity and mortality. The combined annual incidence of ARF and acute-on-chronic renal failure is 2,147 pmp, with a reported overall mortality as high as 50% (8). SC-based kidney regeneration may be critical to reduce the incidence and severity of renal diseases (9).

B. Mazzinghi and E. Ronconi contributed equally to this paper.

Several studies have examined the possibility that BM-derived SCs (BMSCs) might be used for renal repair (9–17). However, these studies disagree on whether there is evidence for BMSC differentiation into renal resident cells, and a recent study even suggests that treatment of renal failure with BMSCs can be offset by a partial maldifferentiation of BMSCs into adipocytes accompanied by glomerular sclerosis (18). Thus, kidney-specific stem/progenitor cells may be better for tissue replacement because of their inherent organ-specific identity, which obviates the risk of maldifferentiation. Although the existence of renal SCs has been an important matter of debate (9,19-24), we recently provided evidence of the existence in the Bowman's capsule of human kidney of a population of renal multipotent progenitors (RMPs) (25). These RMPs are characterized by the expression of two SC markers, CD24 and CD133, which allows their isolation by flow cytometry for clinical purposes (25). When injected into mice models of ARF, RMPs displayed regenerative potential and significantly improved renal function (25). The comprehension of mechanisms that mediate RMP migration, homing, and repopulation in ex vivo treatments are crucial for the success of a clinical strategy of SC-based kidney regeneration.

In this study, to identify RMP homing factors, the chemokine receptor expression pattern of these cells was investigated. Our results demonstrate that RMPs exhibit high expression of the two receptors for SDF-1, CXCR4, and CXCR7, and that both of these receptors are required for therapeutic homing of RMPs in SCID models of ARF by regulating transendothelial migration and survival of i.v. injected RMPs in a nonredundant manner, with important implications for the setup of SC-based therapies.

RESULTS

Human RMPs express high levels of CXCR4 and CXCR7

To determine the mechanisms involved in the therapeutic homing of RMPs into the injured kidney, we first assessed on these cells the expression of mRNA for cc, CXC, and CX3C chemokine receptors by using real-time quantitative RT-PCR. RMPs exhibited high expression of the transcripts for CXCR4 and CXCR7 and lower expression of CXCR3-B, whereas transcripts for CXCR1, CXCR2, CXCR3-A, CXCR5, CXCR6, CCR1, CCR2, CCR3, CCR4, CCR5, CCR6, CCR7, CCR8, CCR9, CCR10, and CX3CR1 were not detectable (Fig. 1 A). Therefore, CXCR4 and CXCR7 protein expression by RMP was assessed by confocal microscopy. CXCR4 protein appeared to be expressed on 95–100% of these cells (Fig. 1 B). Likewise, CXCR7 protein expression could be detected on RMPs by using two different anti-CXCR7 antibodies (Fig. 1, C and D). Because it is known that CXCR7 mRNA expression frequently does not correlate with protein expression, and antibody specificity has been a topic of debate on CXCR7 (7), to further confirm that RMPs expressed both CXCR4 and CXCR7 on their surface, a comprehensive competition binding assay was performed (7). Using ^{125}I-SDF-1 as the "signature" ligand, displacement curves obtained by increasing concentrations

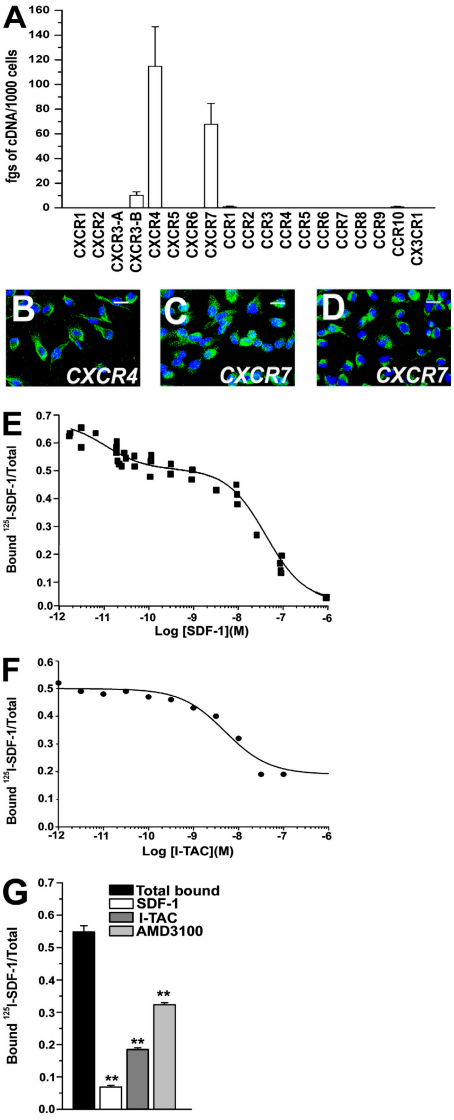

Figure 1. RMPs express CXCR4 and CXCR7. (A) Assessment of mRNA levels for chemokine receptors by real-time quantitative RT-PCR in cultures of RMPs. Results are expressed as the mean ± the SEM of triplicate assessments in primary cultures from 10 different donors. (B) Laser confocal microscopy demonstrates CXCR4 protein expression by RMPs (green). (C and D) Laser confocal microscopy demonstrates CXCR7 protein expression by RMPs (green) by using two polyclonal antibodies recognizing distinct portions of the receptor. To-Pro-3 counterstains nuclei. Bar, 20 μm. (E) Binding of ^{125}I-SDF-1 to RMPs in the presence of increasing concentrations of unlabeled SDF-1. Data show simultaneous analysis of three distinct self-displacement curves. (F) Binding of ^{125}I-SDF-1 to RMPs can be displaced by increasing concentrations of unlabeled I-TAC revealing a typical CXCR7 binding profile. Data are representative of simultaneous analysis of three distinct self displacement curves. (G) ^{125}I-SDF-1 binding to RMPs is completely inhibited by unlabeled SDF-1. Coexpression of CXCR7 and CXCR4 on the surface of RMPs is defined by the partial inhibition of the ^{125}I-SDF-1 binding after complete displacement with cold I-TAC or with the CXCR4 antagonist AMD3100 (50 μM). Data represent the mean ± the SEM, as obtained in three separate experiments. **, $P < 0.001$.

of unlabeled SDF-1 demonstrated specific binding to RMPs (Fig. 1 E). To further confirm the presence of the CXCR7 binding site, ^{125}I-SDF-1 heterologous displacement curves were obtained with increasing concentrations of cold interferon-induced T cell α chemoattractant (I-TAC), a chemokine that shares selective binding of CXCR7 with SDF-1. I-TAC partially displaced ^{125}I-SDF-1 binding, which is in agreement with the presence of both CXCR7 and CXCR4 on the surface of RMPs (Fig. 1 F). In addition, the binding of ^{125}I-SDF-1 to RMPs was only partially inhibited by pretreatment of the cells with the selective CXCR4 antagonist AMD3100 (Fig. 1 G), further confirming the presence of both CXCR4 and CXCR7 on the surface of RMPs.

SDF-1 expression is up-regulated in kidneys with ARF induced by rhabdomyolysis

The high expression of both CXCR4 and CXCR7 on the great majority of RMPs allowed us to hypothesize that their ligand, SDF-1, may be involved in the therapeutic homing of these cells via its interaction with one or both SDF-1 receptors. To support this possibility, we first assessed SDF-1 expression in renal tissues obtained from mice with rhabdomyolysis-induced ARF. Mice were treated with glycerol injection, and a double label immunofluorescence for SDF-1 and the cytoskeletal marker phalloidin was performed at different time points. Phalloidin staining was used inasmuch as the absence or reduction of this marker allows the identification of the necrotic areas (16). Whereas in kidneys obtained from healthy mice before glycerol injection, SDF-1 expression was only observed in some cells within glomerular structures (Fig. 2 A), intense SDF-1 expression was found in ECs, as well as in tubular structures surrounding the areas of tubular necrosis in mice with ARF (Fig. 2, B and C). SDF-1 appeared to be detectable within the first 24 h after glycerol injection, and its expression peaked between 48 and 72 h (Fig. 2, B and C). In the subsequent days, SDF-1 expression was rapidly down-regulated, and starting at day 10 after injury, its expression became comparable to that observed in healthy mice (Fig. 2 D). To assess whether SDF-1 expression correlated with exposure to hemoglobin and myoglobin, primary cultures of mouse renal proximal tubular cells (RPTECs) were treated with 100 ng/ml of hemoglobin or myoglobin for 24 h. Marked SDF-1 mRNA and protein expression occurred in RPTECs after their exposure to hemoglobin or myoglobin (Fig. 2, E and F), thus accounting for the strong up-regulation of SDF-1 observed in kidneys of mice with rhabdomyolysis-induced ARF.

Neutralization of either CXCR4 or CXCR7 inhibits tissue regeneration and renal function improvement in kidneys of SCID mice with ARF

To assess whether the interaction of SDF-1 with CXCR4 and/or CXCR7 was involved in the regenerative capacity of RMPs, mice were injected with RMPs or with saline. Unlike the model reported in our previous study, in which RMP cells were injected at the peak of injury (3 and 4 d after glycerol injection) (25), in the experiments reported herein, RMP cells were injected earlier, i.e., 4 and 20 h after glycerol injection. Measurement of blood urea nitrogen (BUN) levels demonstrated that mice undergoing early treatment with RMPs showed a significantly reduced severity of ARF and a complete recovery of renal function that was not observed in mice treated with saline (Fig. 3 A). In comparison to the previously reported model (25), the early injection of RMPs resulted in a significant reduction of the severity of ARF, as revealed by the consistently lower BUN levels and smaller necrotic areas on day 4 (Fig. 3, A and B). Accordingly, a significant reduction in phalloidin fluorescent staining was observed

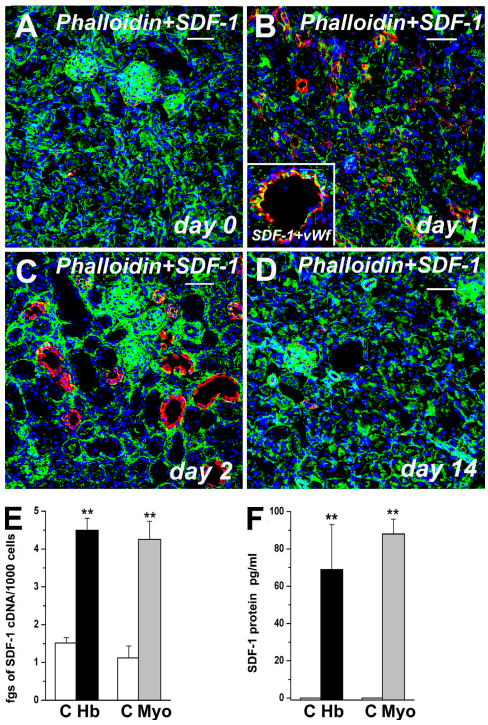

Figure 2. Exposure to hemoglobin and myoglobin up-regulates SDF-1 expression in rhabdomyolysis-induced ARF. (A) Expression of SDF-1 (red) in a healthy mouse kidney stained with the cytoskeleton marker phalloidin (green). (B) Expression of SDF-1 (red) in the kidney of a mouse affected by rhabdomyolysis-induced ARF 24 h after injection of glycerol, and stained with the cytoskeleton marker phalloidin (green). (inset) High-power magnification of a vessel showing SDF-1 staining (red) and vWf (green). (C) Expression of SDF-1 (red) in the kidney of a mouse affected by rhabdomyolysis-induced ARF 48 h after injection of glycerol, and stained with the cytoskeleton marker phalloidin (green). (D) Expression of SDF-1 (red) in the kidney of a mouse affected by rhabdomyolysis-induced ARF 14 d after injection of glycerol, and stained with the cytoskeleton marker Phalloidin (green). To-Pro-3 counterstains nuclei. Bar, 50 μm . (E) Assessment by real-time quantitative RT-PCR of SDF-1 mRNA expression in primary cultures of murine RPTEC before and after exposure to 100 ng/ml hemoglobin or myoglobin. Results are expressed as the mean ± the SEM of three independent experiments. (F) Assessment by ELISA of SDF-1 protein expression in primary cultures of murine RPTECs before and after exposure to 100 ng/ml hemoglobin or 100 ng/ml myoglobin. Results are expressed as the mean ± the SEM of three independent experiments.

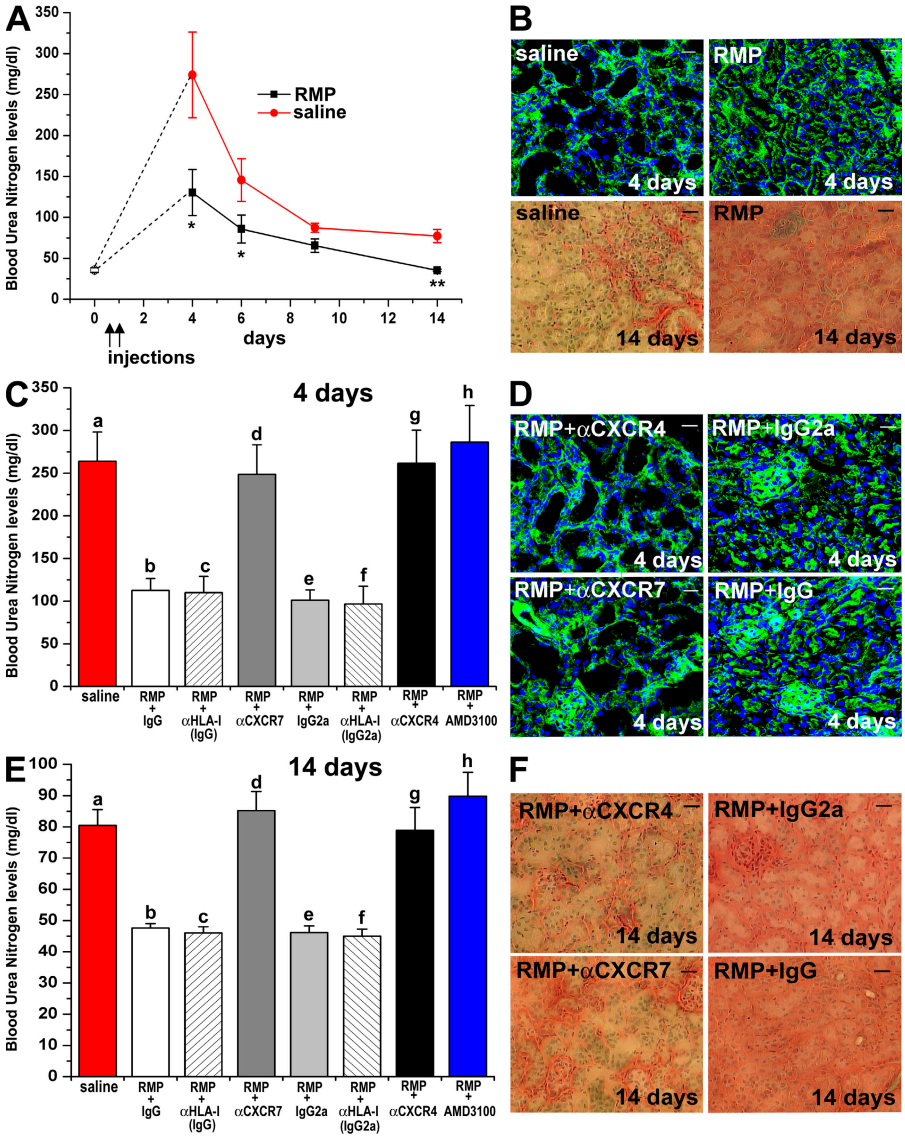

Figure 3. Both CXCR7 and CXCR4 are required for the therapeutic effect of RMPs in ARF. (A) BUN levels as measured in untreated (○) or in glycerol-treated mice that received saline (red circles), or RMPs (filled squares). Black arrows point to the days of saline or RMP injection. *, $P < 0.05$ and **, $P < 0.001$ versus glycerol plus saline. $n = 10$ at each time point. (B; top) Representative micrographs of kidneys from mice treated with saline or with RMPs and stained with phalloidin (day 4). (bottom) Representative micrographs of kidneys from mice treated with saline or with RMPs and stained with Masson's trichrome (day 14). (C) Comparison of BUN levels at day 4 among mice treated with saline, RMP + IgG-Isotype control, RMP + IgG-anti-HLA-I, RMP + anti-CXCR7 antibody, RMP + IgG2a-Isotype control, RMP + IgG2a-anti-HLA-I, RMP + anti-CXCR4 antibody, and RMP + AMD3100. n = at least 10 for each treatment. a vs. b, a vs. e, e vs. g, e vs. h: $P < 0.001$; a vs. c, a vs. f, b vs. d, c vs. d, b vs. h, c vs. h, f vs. g, f vs. h: $P < 0.05$; a vs. d, a vs. g, a vs. h, b vs. e, c vs. e, e vs. f, b vs. c, b vs. f, c vs. f, d vs. g, d vs. h: NS. (D) Representative micrographs of kidneys from mice treated with RMP + IgG2a-Isotype control, RMP + anti-CXCR4, RMP + IgG-Isotype control or RMP + anti-CXCR7, and stained with phalloidin (day 4). (E) Comparison of BUN levels at day 14 among mice treated with saline, RMP + IgG-Isotype control, RMP + IgG-anti-HLA-I, RMP + anti-CXCR7 antibody, RMP + IgG2a-Isotype control, RMP + IgG2a-anti-HLA-I, RMP + anti-CXCR4 antibody, RMP + AMD3100. n = at least 10 for each treatment. a vs. b, a vs. c, a vs. e, a vs. f, b vs. d, b vs. h, c vs. d, c vs. h, e vs. g, e vs. h, f vs. h: $P < 0.001$; f vs. g: $P < 0.05$; a vs. d, a vs. g, a vs. h, b vs. c, b vs. e, c vs. e, c vs. f, e vs. f, d vs. g, d vs. h, g vs. h: NS. (F) Representative micrographs of kidneys from mice treated with RMP + IgG2a-Isotype control, RMP + anti-CXCR4, RMP + IgG-Isotype control, or RMP + anti-CXCR7, and stained with Masson's trichrome (day 14). Data represent the mean values ± the SEM. Bars, 20 μm.

in mice treated with saline in comparison to mice treated with RMPs (63,779 ± 5,608 vs. 138,900 ± 12,876; $P < 0.05$). In addition, evaluation of residual fibrosis with Masson's trichrome staining on day 14 showed that mice treated with saline exhibited focal, but large, areas of interstitial fibrosis, whereas kidney sections of mice injected with RMPs usually showed normal renal morphology (fibrosis score: 2.71 ± 0.18 vs. 0.45 ± 0.15; $P < 0.001$; Fig. 3 B).

RMPs labeled with the red fluorescent dye PKH26 were injected into the tail vein of glycerol-treated SCID mice after pretreatment with a neutralizing anti-CXCR4 antibody, or anti-CXCR7 antibody, or their respective isotype-matched antibodies with irrelevant specificity. To exclude the possibility that circulating RMPs after their coating with antibody were simply removed from the circulation, two different experimental approaches were used. First, two other groups of mice were injected with RMPs pretreated with an isotype-matched antibody that bind to an unrelated surface molecule such as HLA-I, which is highly expressed on the surface of RMPs, as also demonstrated in our previous study (25). Second, the effects of injection of RMPs pretreated with the selective CXCR4 antagonist AMD3100 were assessed. BUN levels, as well as areas of necrosis found 4 d after injury, were significantly higher in mice injected with saline or with PKH26-stained RMPs pretreated with either an anti-CXCR4 or -CXCR7 antibody in comparison with those found in mice injected with PKH26-stained RMPs, which had been pretreated with the respective isotype-matched antibody with irrelevant specificity or the anti–HLA-I antibody, but comparable to those of mice injected with the CXCR4 antagonist AMD3100 (Fig. 3, C and D). Accordingly, a significant reduction in phalloidin staining was observed in mice injected with RMPs pretreated with an anti-CXCR4 antibody (mean fluorescence: 47,825 ± 5,822 vs. 151,680 ± 16,862; $P < 0.05$ or 47,825 ± 5,822 vs. 137,221 ± 23,443; $P < 0.05$) or in mice injected with RMPs pretreated with an anti-CXCR7 antibody (52,736 ± 3,583 vs. 147,492 ± 22,168; $P < 0.05$ or 52,736 ± 3,583 vs. 155,654 ± 27,556; $P < 0.05$) in comparison with the respective control mice injected with PKH26-stained RMPs, which had been pretreated with isotype-matched antibody with irrelevant specificity or the HLA-I antibody. In addition, on day 14 after injury, mice injected with RMPs pretreated with an anti-CXCR4 or -CXCR7 antibody displayed BUN levels significantly higher in comparison with those of mice injected with PKH26-stained RMPs, which had been pretreated with isotype-matched control antibody with irrelevant specificity or the anti–HLA-I antibody, but comparable to those of mice injected with the RMPs pretreated with CXCR4 antagonist AMD3100 (Fig. 3 E). Accordingly, evaluation of the fibrosis score with Masson's trichrome staining in mice injected with RMPs pretreated with an anti-CXCR4 antibody (fibrosis score, 2.57 ± 0.18 vs. 0.32 ± 0.17; $P < 0.001$; or 2.57 ± 0.18 vs. 0.29 ± 0.22; $P < 0.001$) or in mice injected with RMPs pretreated with an anti-CXCR7 antibody (fibrosis score, 2.83 ± 0.18 vs. 0.58 ± 0.22; $P < 0.001$ or 2.74 ± 0.11 vs. 0.54 ± 0.34; $P < 0.001$) demonstrated a higher fibrosis score in comparison with the respective control mice injected with PKH26-stained RMPs, which had been pretreated with isotype-matched control antibody with irrelevant specificity or the HLA-I antibody (Fig. 3 F).

Neutralization of either CXCR4 or CXCR7 reduces the number of RMPs engrafted in kidneys with ARF

To further investigate the mechanisms of activity of SDF-1–CXCR4 and/or SDF-1–CXCR7 interaction, the number of PKH26-labeled cells in the kidney of mice injected with RMPs after pretreatment with a neutralizing anti-CXCR4, anti-CXCR7, or their isotype-matched control antibody with irrelevant specificity, or the HLA-I antibody, was evaluated. Quantitation of the number of PKH26-labeled cells over the total number of renal cells demonstrated a significantly higher percentage of PKH26-labeled cells in the kidney of mice injected with RMPs pretreated with the isotype-matched control antibody with irrelevant specificity or with the isotype-matched anti–HLA-I antibody in comparison with mice injected with RMPs pretreated with an anti-CXCR4 antibody 4 d after injury (8.24 ± 2.1% vs. 0.8 ± 0.43%; **, $P < 0.001$; or 7.32 ± 1.9% vs. 0.8 ± 0.43%; **, $P < 0.001$), as well as 14 d after injury (7.48 ± 1.95% vs. 0.4 ± 0.31%; **, $P < 0.001$; or 8.43 ± 1.77% vs 0.4 ± 0.31%; **, $P < 0.001$; Fig. 4, A, B, and E). In addition, mice injected with RMPs pretreated with the CXCR4 antagonist AMD3100 demonstrated percentages of PKH26-labeled cells comparable to those observed in the kidney of mice injected with RMPs pretreated with an anti-CXCR4 antibody 4 d after injury (0.7 ± 0.34% vs. 0.8 ± 0.43%; NS), as well as on day 14 (0.6 ± 0.38% vs. 0.4 ± 0.31%; NS; Fig. 4 E). Likewise, quantitation of the number of PKH26-labeled cells over the total number of renal cells demonstrated a significantly higher percentage of PKH26-labeled cells in the kidney of mice injected with RMPs pretreated with the isotype-matched antibody with irrelevant specificity or the isotype-matched anti–HLA-I antibody in comparison with mice injected with RMPs pretreated with an anti-CXCR7 antibody (8.68 ± 2.1% vs. 0.38 ± 0.16%; $P < 0.001$ or 7.92 ± 2.4% vs. 0.38 ± 0.16%; **, $P < 0.001$) on day 4 after injury, as well as on day 14 (6.9 ± 1.4% vs. 0.65 ± 0.41%; **, $P < 0.001$; or 7.4 ± 1.34% vs. 0.65 ± 0.41%; **, $P < 0.001$; Fig. 4, C, D, and F). These findings demonstrate that the interaction between SDF-1 with both CXCR4 and CXCR7 expressed by RMPs is involved in their therapeutic homing in injured kidneys.

RMP chemotaxis is selectively mediated through CXCR4, but CXCR7 is required for their transendothelial migration and mediates their adhesion to ECs

It has already been shown that the SDF-1–CXCR4 interaction is important for homing and engraftment of HSCs (2–7, 26, 27), whereas the role of SDF-1–CXCR7 interaction on these processes is unknown. We therefore hypothesized that SDF-1 could act as a chemotactic agent for homing and engraftment of RMPs in injured kidneys via its interaction with CXCR4, CXCR7, or both. To this end, the in vitro chemotactic activity of SDF-1 on RMPs was evaluated. As shown in Fig. 5 A, SDF-1 induced chemotaxis of RMPs in a dose-dependent manner, with maximal chemotactic response detectable at 10–100 nM SDF-1. Little or no migration to the bottom chamber was noted with 10 nM SDF-1 placed in the top and bottom chambers, or in the top chamber only, thus demonstrating that SDF-1 was chemotactic rather than chemokinetic for RMPs (unpublished data). Of note, pretreatment of RMPs with an

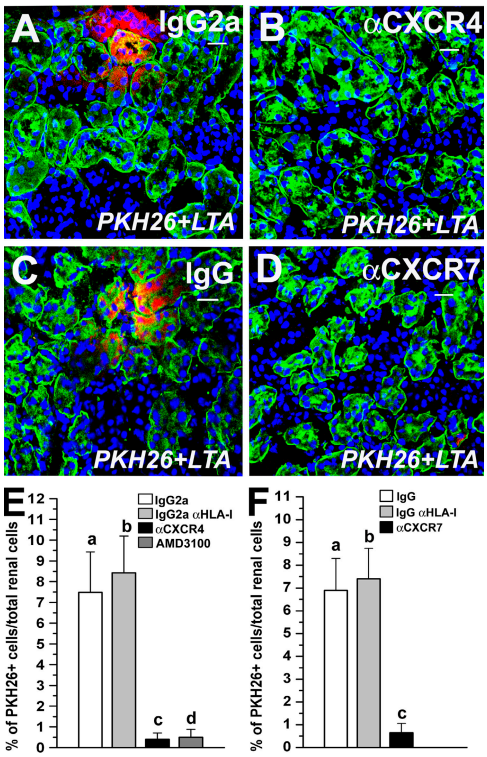

Figure 4. Both CXCR4 and CXCR7 are required for RMP recruitment and engraftment into injured renal tissue. (A) Representative micrograph of kidney sections of mice with induced ARF injected with PKH26-labeled RMPs (red) pretreated with an IgG2a-isotype control antibody and stained with LTA (green) on day 14. (B) Representative micrograph of kidney sections of mice with induced ARF injected with PKH26-labeled RMPs (red) pretreated with an anti-CXCR4 antibody and stained with LTA (green) on day 14. (C) Representative micrograph of kidney sections of mice with induced ARF injected with PKH26-labeled RMP (red) + IgG-isotype control antibody and stained with LTA (green) on day 14. (D) Representative micrograph of kidney sections of mice with induced ARF injected with PKH26-labeled RMPs (red) pretreated with an anti-CXCR7 antibody and stained with LTA (green) on day 14. To-Pro-3 counterstains nuclei. Bars, 20 μm. (E) Quantitative comparison of the number of PKH26-labeled cells over the total number of tissue cells between kidneys obtained from mice treated with PKH26-labeled RMP + IgG2a-isotype control antibody, PKH26-labeled RMP + IgG2a-anti-HLA-I antibody, PKH26-labeled RMP + AMD3100, or PKH26-labeled RMP + anti-CXCR4 antibody on day 14 after glycerol injection. a vs. b, c vs. d: NS; a vs. c, b vs. c, a vs. d, b vs. d: $P < 0.001$. (F) Quantitative comparison of the number of PKH26-labeled cells over the total number of tissue cells between kidneys obtained from mice treated with PKH26-labeled RMP + IgG-isotype control antibody, PKH26-labeled RMP + IgG-anti-HLA-I antibody, or PKH26-labeled RMP + anti-CXCR7 antibody on day 14 after glycerol injection. a vs. b: NS; a vs. c, b vs. c: $P < 0.001$.

anti-CXCR4 neutralizing antibody completely blocked the chemotactic response of RMPs (Fig. 5 B), whereas pretreatment of RMPs with an anti-CXCR7 neutralizing antibody had no effect on their chemotactic response (Fig. 5 B). Collectively, these results suggest that of the two SDF-1 receptors, only CXCR4 is responsible for the migratory response of RMPs.

However, because RMP engraftment into injured renal tissues also requires transendothelial migration, the contribution of CXCR4 and CXCR7 to the SDF-1–induced transendothelial migration via a confluent human umbilical vein EC (HUVEC) monolayer was also assessed. To this end, RMPs were labeled with the fluorescent dye PKH26 and added to transwell culture plates previously cultured with HUVEC monolayers. To evaluate the transmigratory potential of a chemokine gradient, 10 nM SDF-1 was added to the bottom chamber. The exposure of RMPs to 10 nM SDF-1 in the bottom chamber significantly increased transendothelial migration, as assessed by counting the number of cells/field (1.7 ± 0.2 vs. 23.7 ± 2.9 cells/field; $P < 0.001$) and by measuring mean fluorescence staining by confocal microscopy (Fig. 5, C–E). As expected, the increase in transendothelial migration was suppressed by an anti-CXCR4 antibody added to the top chamber, but not by an equal concentration of an isotype-matched control antibody (3.2 ± 0.2 vs. 22 ± 3 cells/field; $P < 0.001$; Fig. 5, C and D). However, the addition of an anti-CXCR7 antibody to the top chamber also completely inhibited transendothelial migration of RMPs, an effect that was not observed in presence of an isotype-matched control antibody (2.2 ± 0.1 vs. 20 ± 1.9 cells/field; $P < 0.001$; Fig. 5, C and E). These findings suggest that the interaction of SDF-1 with CXCR4 is responsible for the recruitment of these cells, but SDF-1–CXCR7 interaction is also required for their transendothelial migration.

To further support the contribution of SDF-1–CXCR7 interaction in the transendothelial migration of RMPs, the role of both CXCR4 and CXCR7 in their adhesion to ECs was examined. It has indeed been reported that SDF-1 can favor the adhesion of SCs to ECs (2–7). To solve this question, RMPs labeled with the red fluorescent dye PKH26 were applied to HUVEC monolayers. A representative image showing PKH26-labeled RMPs (red) adhesion to the EC monolayer stained with Ulex Europeus 1 Lectin (green) is shown in Fig. 5 F. Pretreatment of PKH26-labeled RMPs with an anti-CXCR7 antibody blocked the adhesion of RMPs to HUVEC monolayers, as assessed by counting the number of cells/field (6.6 ± 0.9 vs. 84 ± 6 cells/field; $P < 0.001$) and by measuring mean fluorescence staining by confocal microscopy (Fig. 5, G and H). In contrast, pretreatment of RMPs with an anti-CXCR4 antibody did not have any effect (87.3 ± 5.2 vs. 89.2 ± 3.7 cells/field; NS; Fig. 5, G and H). Collectively, these results suggest that CXCR7, but not CXCR4, mediates adhesion of RMPs to ECs, and is therefore responsible for their transendothelial migration.

CXCR7, but not CXCR4, is responsible for RMP survival

It has been shown that HSCs from adult subjects depend upon SDF-1 not only for their migration/homing, but also for their survival and proliferation (2–7). We therefore investigated the effects of SDF-1 on the survival/proliferation of RMPs. SDF-1 exhibited a limited effect on DNA synthesis under basal conditions, but it significantly enhanced the survival/proliferation of RMPs cultured in presence of H_2O_2 (Fig. 6 A).

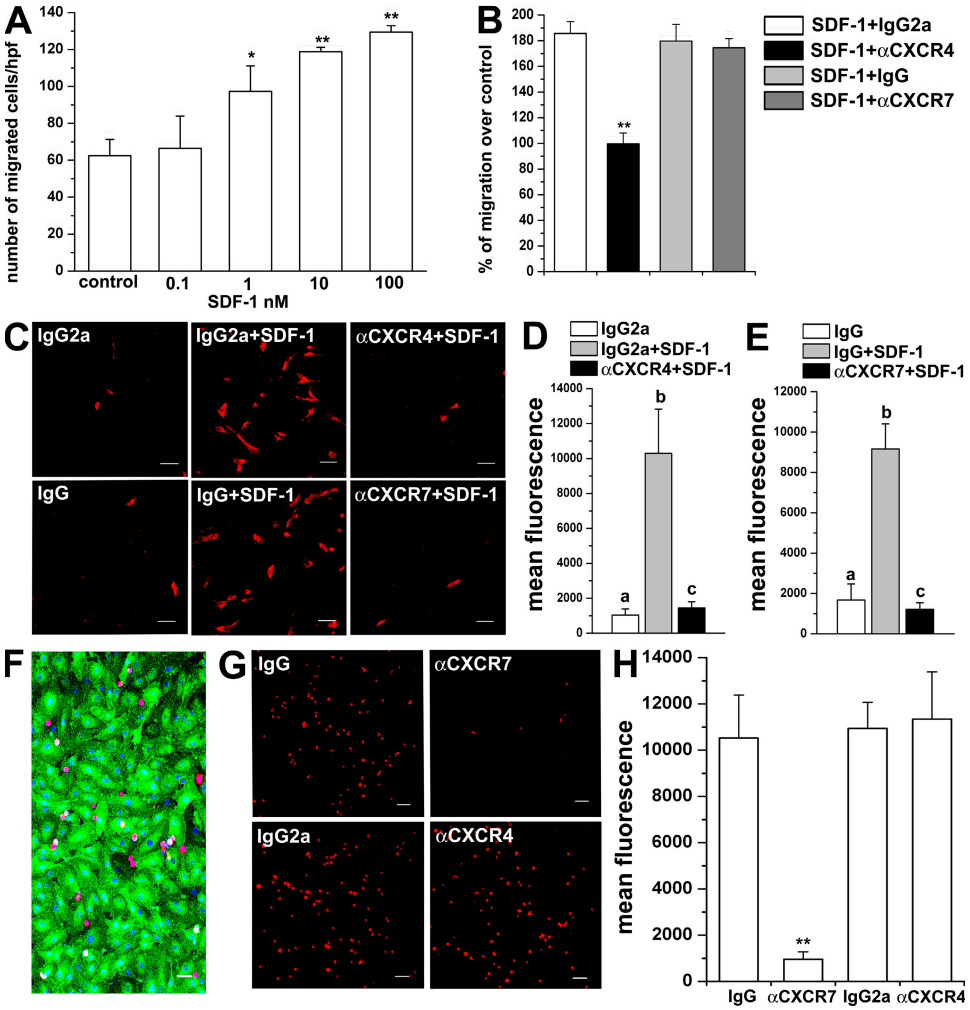

Figure 5. RMP migration is mediated through CXCR4, but CXCR7 is required for transendothelial migration and mediates EC adhesion. (A) Dose-dependent migration of RMPs in response to SDF-1. Results are expressed as the mean ± the SEM of triplicate assessment. One representative of three independent experiments is shown. *, $P < 0.05$; **, $P < 0.001$. (B) RMP migration is reverted by pretreatment with anti-CXCR4 neutralizing antibody, but not by an anti-CXCR7 neutralizing antibody. Results are expressed as the mean ± the SEM as assessed in four independent experiments. **, $P < 0.001$. (C) Transendothelial migration of RMPs is reverted by pretreatment with either an anti-CXCR4 or an anti-CXCR7 neutralizing antibody. One representative of three independent experiments is shown. (D) Quantitation of transendothelial migration of RMPs. Results are expressed as the mean ± the SEM of fluorescence intensity as observed in four independent experiments. a vs. b and b vs. c: $P < 0.05$; a vs. c: NS. (E) Quantitation of transendothelial migration of RMPs. Results are expressed as the mean ± the SEM of fluorescence intensity as observed in four independent experiments. a vs. b and b vs. c: $P < 0.05$; a vs. c: NS. (F) HUVECs were stained with Ulex europeus I lectin (green) to visualize the EC monolayer. To-Pro-3 was used to counterstain nuclei. (G) PKH26-labeled RMPs (red) were cultured in presence or absence of an isotype control antibody, an anti-CXCR7 antibody or an anti-CXCR4 neutralizing antibody. One representative of three independent experiments is shown. (H) Quantitation of RMP adhesion to HUVEC monolayers. Results are expressed as the mean ± the SEM of fluorescence intensity as observed in four independent experiments. **, $P < 0.001$. Bars; (C and F) 50 μm; (G) 100 μm.

To evaluate whether the SDF-1–mediated increase of DNA synthesis was related to a reduction of apoptosis, the amount of DNA fragmentation on RMPs treated with H_2O_2 in the presence or absence of increasing concentrations of SDF-1 (1–100 nM) was assessed by using the TUNEL technique, and apoptotic cells were quantified by counting their percentages over the total number of cells, as well as by measuring mean fluorescence of TUNEL staining by confocal microscopy. The addition in RMP cultures of H_2O_2 up-regulated DNA fragmentation, an effect that was completely reverted in presence of 10 nM SDF-1 (47 ± 12% vs. 0.7 ± 0.3%; $P < 0.001$; and mean fluorescence 12,738 ± 1,534 vs. 281.5 ± 57; $P < 0.001$; Fig. 6 B). Blocking the CXCR4 receptor with an anti-CXCR4 mAb did not display any effect on either SDF-1–mediated enhancement of RMP survival/proliferation, as assessed by evaluation of [^{3}H]thymidine incorporation (Fig. 6 C) or the percentage of apoptotic cells in comparison with cells treated with the isotype-matched control antibody, as assessed by the TUNEL technique (0.3 ± 0.6% vs. 0.9 ± 0.1%; NS; mean fluorescence, 210 ± 48.76 vs. 204.7 ± 50.5; NS; Fig. 6 D).

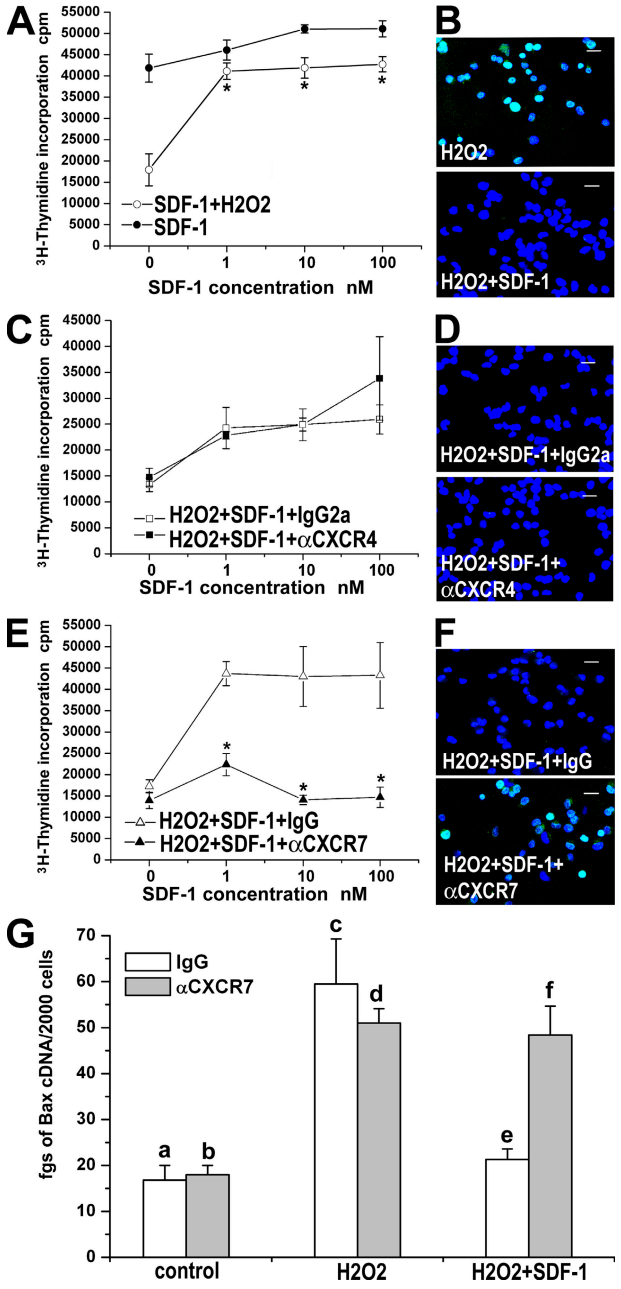

Figure 6. Effect of SDF-1 on RMP survival is mediated by CXCR7, but not by CXCR4. (A) SDF-1 up-regulates DNA synthesis in basal conditions and rescues DNA synthesis after H_2O_2 treatment. Results are expressed as the mean ± the SEM of triplicate assessment, as assessed in four independent experiments. (B) A representative micrograph of TUNEL immunostaining demonstrates that SDF-1 rescues apoptosis (green) induced by H_2O_2 treatment. One representative of three independent experiments is shown. To-Pro-3 counterstains nuclei. (C) Lack of effect of a neutralizing anti-CXCR4 antibody on SDF-1–mediated prosurvival effect. Results are expressed as the mean ± the SEM of triplicate assessment, as assessed in four independent experiments. (D) A representative micrograph of TUNEL immunostaining (green) demonstrates that SDF-1–mediated rescue from apoptosis induced by H_2O_2 treatment is not neutralized by an anti-CXCR4. One representative of three independent experiments is shown. To-Pro-3 counterstains nuclei. (E) A neutralizing anti-CXCR7 antibody reverts the prosurvival effect of SDF-1. Results are expressed as the mean ± the SEM of triplicate assessment, as assessed in four independent experiments. (F) A representative micrograph of TUNEL immunostaining (green) demonstrates that SDF-1–mediated rescue from apoptosis induced by H_2O_2 treatment is completely reverted by an anti-CXCR7 antibody. One representative of three independent experiments is shown. To-Pro-3 counterstains nuclei. (G) The SDF-1-CXCR7 axis modulates Bax transcription in response to H_2O_2. Results are expressed as the mean ± the SEM of triplicate assessment, as assessed in four independent experiments. a vs. c, e vs. f, c vs. e, b vs. d, b vs. f: $P < 0.05$; a vs. b, c vs. d, d vs. f: NS. Bars, 20 μm.

In contrast, treatment of RMPs with an anti-CXCR7 antibody completely reverted the SDF-1–mediated stimulation of DNA synthesis (Fig. 6 E) and increased the percentage of apoptotic cells in comparison with cells treated with the isotype-matched control antibody (35 ± 2.6% vs. 0.8 ± 0.4%; $P < 0.001$; Fig. 6 F), the mean fluorescence being 15,467 ± 3,445 vs. 272.6 ± 49.3; $P < 0.001$. In addition, although H_2O_2 addition was associated with increased mRNA levels of the proapoptotic gene Bax-2, the addition of SDF-1 to RMPs treated with H_2O_2 restored Bax-2 basal levels, an effect that was completely reverted by an anti-CXCR7 (Fig. 6 G), but not by an anti-CXCR4 antibody (not depicted). Collectively, these results indicate that SDF-1 enhances RMP survival through its interaction with CXCR7, whereas the SDF-1–CXCR4 interaction is not involved in this process.

DISCUSSION

Cells can reach specific target tissues through the general circulation by different mechanisms. Homing has been studied extensively both in vitro and in vivo with different cell types, such as leukocytes or HSCs (2–7, 26-29), and it is believed to rely on adhesion molecules and chemokine receptors via a multistep cascade, consisting of a rolling process followed by firm adhesion and transendothelial migration into the surrounding tissue (2–7, 26–32). The repertoire and the level of chemokine expression by the target tissue, as well as expression of the respective receptors on SCs, influence the efficiency of homing (2–7). The critical role of SDF-1 in HSC homing has been suggested by several studies (2–7). Accordingly, it had been demonstrated that SDF-1 regulates trafficking of $CD34^+$ hematopoietic stem/progenitor cells, as well as pre–B and T lymphocytes (2–7). However, in recent years, evidence has been accumulated to suggest that SDF-1 is also a crucial regulator of SC biology in several tissue-committed stem/progenitor cells, such as primordial germ cells, skeletal muscle satellite progenitor cells, neural SCs, liver oval SCs, and retinal pigment epithelium progenitors (3–5).

In humans, RMPs have recently been characterized as a population of cells localized at the urinary pole of the Bowman's capsule that can differentiate into tubular cells of different portions of the nephron (25). When injected i.v., human RMPs have been shown to induce a complete recovery of both renal structure and function in rhabdomyolysis-induced ARF of SCID mice (25). The reason for the therapeutic effect of RMPs is likely to be ascribed to the ability of these cells to

reach and colonize the kidney, depending in turn on EC adhesion and extravasation.

In this study, we demonstrate that among all known chemokine receptors, RMPs exhibited high expression of the two receptors for SDF-1, CXCR4, and CXCR7, which suggests that these cells may be responsive to the activity of this chemokine. Indeed, not only did RMPs express mRNA and protein for both receptors, but they also reacted with SDF-1 according to a two-site binding model (7). Notably, this binding was only partially inhibited by cell pretreatment with a selective CXCR4 antagonist and partially displaced by I-TAC, which is in agreement with previously reported results showing the ability of CXCR7 to bind both SDF-1 and I-TAC (7). Moreover, we observed an increased expression of SDF-1 in renal ECs and epithelial cells surrounding injured tubular structures, which is in agreement with SDF-1 up-regulation reported in ischemia/reperfusion-induced ARF in rats (33). In our model, up-regulation of SDF-1 expression and production was related to the exposure of these cells to toxic amounts of hemoglobin and myoglobin resulting from rhabdomyolysis. A similar effect may also occur in human pathological conditions, resulting in ARF related to acute and massive red blood cells and skeletal muscle cell destruction. When human RMPs were injected into SCID mice on the same day as the injury, there was a substantial reduction of the severity of ARF and a complete recovery of renal function in comparison with mice treated with saline. In agreement with a central role of SDF-1 in RMP therapeutic homing to injured renal tissue, neutralization of CXCR4 completely blocked the regenerative capacity of RMPs, caused by a substantially decreased recruitment of these cells in injured renal tissue. Surprisingly, however, both the in vivo regenerative capacity of RMPs and their engraftment in injured kidneys was also abolished when these cells were injected with a neutralizing anti-CXCR7 antibody, suggesting that not only CXCR4 but also CXCR7 expression is critical for the therapeutic homing of RMPs in injured renal tissue. These antibody-mediated inhibitory effects did not simply reflect the removal of antibody-coated RMPs from the circulation. Indeed, no inhibitory effects were obtained by using the same cells pretreated with antibody specific for HLA-I, which is a molecule that is highly expressed on the surface of RMPs (25). More importantly, RMP cells pretreated with AMD3100, which is a selective antagonist of CXCR4, exhibited effects quite comparable to those exerted by RMP cells pretreated with anti-CXCR4 or -CXCR7 antibody.

To understand the respective roles of CXCR4 and CXCR7 on the regenerative activity of RMPs, the migration of RMPs was evaluated in vitro by a transwell assay, which was already proven as a reliable indicator of the mechanisms that govern cellular trafficking in vivo (34). Only blocking of CXCR4, but not of CXCR7, inhibited the chemotactic activity of SDF-1 on RMPs, suggesting that only CXCR4 was required for the recruitment of human RMP. However, when the transendothelial migration of RMPs via a confluent HUVEC monolayer in response to SDF-1 was assessed, blocking of either CXCR4 or CXCR7 appeared to be inhibitory, suggesting that CXCR7 was in some way involved in the process of migration at the endothelial level. This possibility was further supported by the observation that only blocking CXCR7, but not CXCR4, inhibited the adhesion of RMPs to ECs in vitro. Thus, it appears that in the therapeutic homing of RMPs in injured kidneys of SCID mice, the SDF-1–CXCR4 interaction is responsible for the recruitment of RMPs, whereas the binding of SDF-1 to CXCR7 is required for RMP adhesion to ECs, and therefore is essential for their transendothelial migration. Interestingly, however, CXCR4 was also involved in transendothelial migration, suggesting that this chemokine receptor probably plays a role by fulfilling an "interceptor" function and regulating the translocation of SDF-1 across the endothelium, as previously demonstrated also in BM-derived endothelium (27).

In previous studies, SDF-1 has also been implicated not only in SC adhesion but also in the induction of SC proliferation/survival (4–7, 34, 35). In addition, SDF-1 was found to be critical for the normal development of several organs, suggesting that this chemokine may play a role in the migration/adhesion/proliferation/survival of most adult progenitor cells (4–6). Interestingly, apoptotic cell death of RMP induced by H_2O_2 can be reverted by treatment with SDF-1. H_2O_2 generated during hypoxia/reoxygenation and ischemia/reperfusion injury is an important mediator of cell death induced during renal ischemia (36, 37), as well as in myohemoglobinuric renal injury (36, 38), suggesting that SDF-1 production might play a critical role in RMP protection after kidney injury. SDF-1 has previously been thought to mediate all its functions exclusively via CXCR4 (4–6). The results of this study clearly demonstrate that, at least in RMP, the survival process induced by SDF-1 is mediated by CXCR7, but not by CXCR4. This finding is consistent with the results of another study suggesting that the survival/antiapoptotic effect of SDF-1 on mesenchymal SCs was not mediated through CXCR4 (35). In addition, some suggestions of discrepant CXCR4 expression and SDF-1 responsiveness already exist in the literature. For example, previous studies demonstrated that adhesion of E11 fetal liver cells to BM endothelium can be neutralized by anti–SDF-1 antibodies, despite the fact that the E11 fetal liver cells do not migrate in response to SDF-1 (39). Collectively, these findings not only provide an explanation for the mechanisms that allow the therapeutic homing of RMPs in injured kidney tissues, but may also require a reexamination of much of the previous work that presumed a mutually exclusive biological interaction between SDF-1 and CXCR4. Indeed, the finding that the adhesion and survival effect of SDF-1 on RMPs was selectively mediated through CXCR7 suggests that CXCR7 might play an important, even if still unexplored, role in other progenitor/SC physiology (2–7, 26–40). A great deal is known about the effects of SDF-1 on SC functions, and this information has been used for modulating these cells in the clinical setting, particularly for enhancing transplantation effectiveness (3). The results of this study suggest that not only CXCR4 but also CXCR7 is required for the efficient

delivery of RMPs to injured kidneys in response to SDF-1 for cell therapy of ARF, a property that might be shared by other types of SCs, with important implications for the set up of SC-based therapies.

MATERIALS AND METHODS

Antibodies. The following antibodies were used: anti-CXCR4 (clone 12G5, mouse IgG2a; R&D Systems), anti-CXCR7 (rabbit polyclonal IgG directed toward the second extracellular domain; Abcam; rabbit polyclonal IgG directed toward the third cytoplasmic loop; Affinity BioReagents), anti-SDF-1 (clone 179018, mouse IgG1; R&D Systems), anti-vWf (polyclonal IgG; Dako), mouse anti–human HLA-I (IgG2a; Sigma-Aldrich), rabbit anti–human HLA-I (IgG; Santa Cruz Biotechnology), mouse IgG2a isotype control (clone 20102; R&D Systems), and rabbit IgG isotype control (R&D Systems). Alexa Fluor 546–labeled goat anti–mouse IgG1, Alexa Fluor 488–labeled goat anti–mouse IgG2a, and Alexa Fluor 488–labeled goat anti–rabbit IgG were obtained from Invitrogen.

Isolation and culture of RMPs. RMPs were obtained as previously described (25) from five patients who underwent radical nephrectomy because of renal cell carcinoma. Macroscopically normal portions of renal tissue were obtained from the pole opposite the tumor, in accordance with the recommendations of the Ethical Committee of the Azienda Ospedaliero-Universitaria Careggi, Florence, Italy on human experimentation.

Cell cultures. Primary cultures of mouse RPTECs were obtained as previously described (41). HUVECs were obtained from Lonza and cultured following manufacturer's instructions.

Confocal microscopy. Confocal microscopy was performed on 5-μm sections of renal frozen tissues or on cells cultured on chamber slides by using a LSM 510 META laser confocal microscope (Carl Zeiss, Inc.), as previously described (42).

Staining with FITC-labeled Ulex europeus I lectin (Sigma-Aldrich), FITC-labeled Lotus tetragonolobus agglutinin (LTA; Vector Laboratories), and Alexa Fluor 488 phalloidin (Invitrogen) were performed following manufacturer's instructions. For quantification of necrosis in glycerol-injected SCID mice, four random fields of kidney tissue stained for phalloidin were recorded from each mouse for each group of treatments at day 4, using a 20× objective. All random scans of the kidney tissue were recorded at the same photomultiplier tube, pinhole aperture, and laser voltage setting and analyzed using LSM 510 confocal microscopy software 3.0.

Real-time quantitative RT-PCR. TaqMan RT-PCR was performed as previously described (25). CXCR1, CXCR2, CXCR5, CXCR6, CXCR7, CX3CR1, CCR1, CCR2, CCR3, CCR4, CCR5, CCR6, CCR7, CCR8, CCR9, CCR10, SDF-1, and Bax quantitation was performed using Assay on Demand kits (Applied Biosystems). CXCR4 primers and probes were as follows: probe VIC 5′-ACACTTCAGATAACTACACCGAGGAAATGGGC-3′, forward: 5′-CACCGCATCTGGAGAACCA-3′, and reverse: 5′-CTTCATGGAGTCATAGTCCCCTG-3′. CXCR3-A and CXCR3-B primers and probes were previously described (43).

Binding assays. Binding assays were performed as previously described (43). In brief, cells were plated in 24-well culture plates and washed twice with washing buffer (0.5 M NaCl, 50 mM Hepes, 1 mM $CaCl_2$, 5 mM $MgCl_2$, and 1% BSA, pH 7.2), and incubated in triplicate in binding buffer (25 mM Hepes, 140 mM NaCl, 1 mM $CaCl_2$, 5 mM $MgCl_2$, and 0.2% BSA, pH 7.1) with a constant concentration (20 pM) of ^{125}I-labeled SDF-1 (PerkinElmer) in the presence of increasing concentrations of unlabeled chemokines, and/or 50 μM of the CXCR4 selective antagonist AMD3100 (Sigma-Aldrich). Incubations took place in 200 μl binding buffer. After incubation at room temperature for 2 h, binding buffer was aspirated and cells were washed once in PBS (without Ca and Mg) and lysed in 0.2 ml 0.5 N NaOH. Radioactivity was determined using a γ counter. Data were analyzed using the computer program Ligand (44).

SDF-1 ELISA assay. Mouse RPTECs were plated in 24-well culture plates (5×10^4 cells/well) and treated with 100 ng/ml of hemoglobin (Sigma-Aldrich) or 100 ng/ml myoglobin (Sigma-Aldrich) for 24 h at 37°C. After incubation, supernatants were collected and RPTEC pellets were recovered to assess SDF-1 protein and mRNA levels. SDF-1 protein was assessed by an immunoenzymatic assay (R&D Systems) following the manufacturer's instructions.

Xenograft in SCID mouse model of ARF. Models of rhabdomyolysis-induced ARF were performed in female SCID mice (Harlan), as previously described (25), by intramuscular injection with hypertonic glycerol (8 ml/kg body wt of a 50% glycerol solution; Sigma-Aldrich) into the inferior hind limbs at day 0. Animal experiments were authorized by Ministero della Salute of Italy (Dipartimento della Sanità Pubblica e Veterinaria) and performed in adherence to the National Institutes of Health Guide for the Care and Use of Laboratory Animals. 9 groups of mice on day 0 received an i.v. injection into the tail vein as follows: group 1, $n = 50$ mice, saline; group 2, $n = 40$ mice, PKH26-stained RMPs (0.75×10^6 cells 4 h after glycerol injection and 0.75×10^6 cells 20 h after glycerol injection); group 3, $n = 30$ mice, PKH26-stained RMPs pretreated with mouse IgG2a isotype control antibody (R&D Systems; 0.75×10^6 cells 4 h after glycerol injection and 0.75×10^6 cells 20 h after glycerol injection); group 4, $n = 30$ mice, PKH26-stained RMPs pretreated with an anti-CXCR4 neutralizing antibody (R&D Systems; 0.75×10^6 cells 4 h after glycerol injection and 0.75×10^6 cells 20 h after glycerol injection); group 5, $n = 30$ mice, PKH26-stained RMPs pretreated with rabbit IgG isotype control antibody (R&D Systems; 0.75×10^6 cells 4 h after glycerol injection and 0.75×10^6 cells 20 h after glycerol injection); group 6, $n = 30$ mice, PKH26-stained RMPs pretreated with an anti-CXCR7 neutralizing antibody (Abcam; 0.75×10^6 cells 4 h after glycerol injection and 0.75×10^6 cells 20 h after glycerol injection); group 7, $n = 20$ mice, PKH26-stained RMPs pretreated with rabbit IgG anti–HLA-I antibody (Santa Cruz Biotechnology; 0.75×10^6 cells 4 h after glycerol injection and 0.75×10^6 cells 20 h after glycerol injection); group 8, $n = 16$ mice, PKH26-stained RMP pretreated with mouse IgG2a anti–HLA-I antibody (Sigma-Aldrich; 0.75×10^6 cells 4 h after glycerol injection and 0.75×10^6 cells 20 h after glycerol injection); and group 9, $n = 20$ mice, PKH26-stained RMPs pretreated with 50 μM AMD3100 (Sigma-Aldrich; 0.75×10^6 cells 4 h after glycerol injection and 0.75×10^6 cells 20 h after glycerol injection). RMPs were labeled with the PKH26 Red Fluorescence Cell Linker kit (Sigma-Aldrich) immediately before injection. Pretreatment with neutralizing antibodies was performed by incubating cells with antibodies (10 μg/10^6 cells) for 30 min on ice. For each group, 30 min after each i.v. injection, mice were treated i.p. with 10 μg/mouse of the respective neutralizing antibody. At least 10 mice were killed for each group of treatment at 4, 6, 9, or 14 d, and BUN levels were measured in heparinized blood by the Aeroset c8000 test (Abbott). Normal range in our experiments was between 30 and 37 mg/dl, as calculated in 10 additional untreated mice (day 0). BUN levels that exceeded 40 mg/dl were considered abnormal.

For evaluation of SDF-1 secretion, ARF was induced in an additional group of 32 mice, as described in the previous paragraph. Mice were killed on day 0, 1, 2, 3, 4, 6, 10, or 14, and their kidneys were removed and stained with phalloidin and SDF-1 ($n = 4$ at each time point).

Renal morphology. 5-μm-thick kidney sections of mice killed at day 14 were fixed in ethanol and stained with a Masson-Goldner trichromic kit (Bio-Optica) to evaluate the fibrosis of cortical interstitium. Nonoverlapping fields of the entire section (up to 20 fields for each mouse) were independently analyzed at high magnification using a 20× objective by two observers. The severity of renal scarring was assessed as follows: normal tubulointerstitium scored 0; mild tubular atrophy with interstitial edema or fibrosis affecting up to 25% of the field scored 1; moderate tubular atrophy with interstitial edema or fibrosis affecting 25–50% of the field scored 2; and severe

tubular atrophy with interstitial edema or fibrosis affecting >50% of the field scored 3.

Chemotaxis assay. Cell migration assays were performed using Boyden chambers (NeuroProbes) with fibronectin-coated polycarbonate membranes (8 μm pore size; NeuroProbes) on 25,000 RMPs, as previously described (45). SDF-1 (Peprotech) was used at a concentration of 0.1–100 nM in endothelial basal medium (EBM) 1% FBS. In some experiments, RMPs were pretreated with a neutralizing anti-CXCR4 (10 μg/ml), an anti-CXCR7 (10 μg/ml) antibody, or with 10 μg/ml of the respective isotype-matched control antibodies. In these experiments, SDF-1 was used at a concentration of 10 nM in EBM 1% FBS.

Transendothelial migration assay. The transendothelial migration assay was conducted in 12-transwell culture plates containing microporous (8.0 μm) membranes (Corning Costar Corp.). In brief, HUVECs were seeded onto transwell culture plates and the confluency of monolayer was verified by Dif-quik staining. RMPs were labeled with PKH26 and added to the top chamber in presence of a neutralizing anti-CXCR7 antibody, an IgG isotype control antibody, a neutralizing anti-CXCR4 antibody, or an IgG2a isotype control antibody (all at a concentration of 8 μg/ml). Transmigration toward a 10-nM SDF-1 gradient was quantified by confocal microscopy on at least 6 20× fields for each filter.

Adhesion assay. HUVECs were allowed to adhere to chamber slides (1.5×10^5/chamber) overnight in EGM-2MV (Lonza) to obtain a monolayer. RMPs (5×10^4 cells/chamber) were labeled with the PKH26 Red Fluorescence Cell Linker kit and pretreated with an anti-CXCR7 antibody, an IgG isotype control antibody, an anti-CXCR4 antibody, or an IgG2a isotype control antibody (all at a concentration of 8 μg/ml) for 30 min on ice, washed, and added to HUVEC monolayers. Adhesion was allowed for 15 min at 37°C. Nonadherent RMPs were thoroughly washed off, and the adhered RMPs were quantified by confocal microscopy on 4 10× fields.

Cell proliferation assay. ^{3}[H]thymidine incorporation was assessed as previously described (42). Cells were cultured with SDF-1 (1–100 nM) and SDF-1 + 850 μM H_2O_2 (Sigma-Aldrich) for 8 h in presence or absence of an anti-CXCR7 antibody, an IgG isotype control antibody, an anti-CXCR4 antibody, or an IgG2a isotype control antibody (all at a concentration of 8 μg/ml).

TUNEL assay. RMPs were cultured with SDF-1 (1–100 nM) and SDF-1 + 850 μM H_2O_2 for 8 h in the presence or absence of an anti-CXCR7 antibody, an IgG isotype control antibody, an anti-CXCR4 antibody, or an IgG2a isotype control antibody (all at a concentration of 8 μg/ml). Apoptotic RMPs were quantified by confocal microscopy on 12 40× fields for each slide.

Statistical analysis. The results are expressed as the mean ± the SEM. Comparison between groups was performed by the Mann-Whitney test or the Wilcoxon test, as appropriate. $P < 0.05$ was considered to be statistically significant.

The research leading to these results has received funding from the European Research Council Starting Grant under the European Community's Seventh Framework Programme (FP7/2007-2013) ERC grant.

This study was supported by the Tuscany Ministry of Health, Ministero dell'Istruzione, dell'Università e della Ricerca (MIUR), Ente Cassa di Risparmio Firenze, and the Associazione Italiana per la Ricerca sul Cancro. B. Mazzinghi and E. Parente are recipients of a Fondazione Italiana per la Ricerca sul Cancro fellowship.

The authors have no conflicting financial interests.

Submitted: 4 September 2007
Accepted: 15 January 2008

REFERENCES

1. Blau, H.M., T.R. Brazelton, and J.M. Weimann. 2001. The evolving concept of a stem cell: entity or function? *Cell*. 105:829–841.
2. Lapidot, T., A. Dar, and O. Kollet. 2005. How do stem cells find their way home? *Blood*. 106:1901–1910.
3. Galvez, B.G., M. Sampaolesi, S. Brunelli, D. Covarello, M. Gavina, B. Rossi, G. Constantin, Y. Torrente, and G. Cossu. 2006. Complete repair of dystrophic skeletal muscle by mesoangioblasts with enhanced migration ability. *J. Cell Biol.* 174:231–243.
4. Romagnani, P., L. Lasagni, B. Mazzinghi, E. Lazzeri, and S. Romagnani. 2007. Pharmacological modulation of stem cell function. *Curr. Med. Chem.* 14:1129–1139.
5. Ratajczak, M.Z., E. Zuba-Surma, M. Kucia, R. Reca, W. Wojakowski, and J. Ratajczak. 2006. The pleiotropic effects of the SDF-1-CXCR4 axis in organogenesis, regeneration and tumorigenesis. *Leukemia*. 20:1915–1924.
6. Kortesidis, A., A. Zannettino, S. Isenmann, S. Shi, T. Lapidot, and S. Gronthos. 2005. Stromal-derived factor-1 promotes the growth, survival, and development of human bone marrow stromal stem cells. *Blood*. 105:3793–3801.
7. Burns, J.M., B.C. Summers, Y. Wang, A. Melikian, R. Berahovich, Z. Miao, M.E. Penfold, M.J. Sunshine, D.R. Littman, C.J. Kuo, et al. 2006. A novel chemokine receptor for SDF-1 and I-TAC involved in cell survival, cell adhesion, and tumor development. *J. Exp. Med.* 203:2201–2213.
8. Ali, T., I. Khan, W. Simpson, G. Prescott, J. Townend, W. Smith, and A. Macleod. 2007. Incidence and outcomes in acute kidney injury: a comprehensive population-based study. *J. Am. Soc. Nephrol.* 18:1292–1298.
9. Little, M.H. 2006. Regrow or repair: potential regenerative therapies for the kidney. *J. Am. Soc. Nephrol.* 17:2390–2401.
10. Prodromidi, E.I., R. Poulsom, R. Jeffery, C.A. Roufosse, P.J. Pollard, C.D. Pusey, and H.T. Cook. 2006. Bone marrow-derived cells contribute to podocyte regeneration and amelioration of renal disease in a mouse model of Alport syndrome. *Stem Cells*. 24:2448–2455.
11. Kunter, U., S. Rong, Z. Djuric, P. Boor, G. Muller-Newen, D. Yu, and J. Floege. 2006. Transplanted mesenchymal stem cells accelerate glomerular healing in experimental glomerulonephritis. *J. Am. Soc. Nephrol.* 17:2202–2212.
12. Sugimoto, H., T.M. Mundel, M. Sund, L. Xie, D. Cosgrove, and R. Kalluri. 2006. Bone-marrow-derived stem cells repair basement membrane collagen defects and reverse genetic kidney disease. *Proc. Natl. Acad. Sci. USA*. 103:7321–7326.
13. Stokman, G., J.C. Leemans, N. Claessen, J.J. Weening, and S. Florquin. 2005. Hematopoietic stem cell mobilization therapy accelerates recovery of renal function independent of stem cell contribution. *J. Am. Soc. Nephrol.* 16:1684–1692.
14. Morigi, M., B. Imberti, C. Zoja, D. Corna, S. Tomasoni, M. Abbate, D. Rottoli, S. Angioletti, A. Benigni, N. Perico, et al. 2004. Mesenchymal stem cells are renotropic, helping to repair the kidney and improve function in acute renal failure. *J. Am. Soc. Nephrol.* 15:1794–1804.
15. Kale, S., A. Karihaloo, P.R. Clark, M. Kashgarian, D.S. Krause, and L.G. Cantley. 2003. Bone marrow stem cells contribute to repair of the ischemically injured renal tubule. *J. Clin. Invest.* 112:42–49.
16. Duffield, J.S., K.M. Park, L.L. Hsiao, V.R. Kelley, D.T. Scadden, T. Ichimura, and J.V. Bonventre. 2005. Restoration of tubular epithelial cells during repair of the postischemic kidney occurs independently of bone marrow-derived stem cells. *J. Clin. Invest.* 115:1743–1755.
17. Lin, F., A. Moran, and P. Igarashi. 2005. Intrarenal cells, not bone marrow-derived cells, are the major source for regeneration in postischemic kidney. *J. Clin. Invest.* 115:1756–1764.
18. Kunter, U., S. Rong, P. Boor, F. Eitner, G. Muller-Newen, Z. Djuric, C.R. van Roeyen, A. Konieczny, T. Ostendorf, L. Villa, et al. 2007. Mesenchymal stem cells prevent progressive experimental renal failure but maldifferentiate into glomerular adipocytes. *J. Am. Soc. Nephrol.* 18:1754–1764.
19. Oliver, J.A., O. Maarouf, F.H. Cheema, T.P. Martens, and Q. Al-Awqati. 2004. The renal papilla is a niche for adult kidney stem cells. *J. Clin. Invest.* 114:795–804.
20. Dekel, B., L. Zangi, E. Shezen, S. Reich-Zeliger, S. Eventov-Friedman, H. Katchman, J. Jacob-Hirsch, N. Amariglio, G. Rechavi, R. Margalit,

and Y. Reisner. 2006. Isolation and characterization of nontubular sca-1+lin- multipotent stem/progenitor cells from adult mouse kidney. *J. Am. Soc. Nephrol.* 17:3300–3314.
21. Bussolati, B., S. Bruno, C. Grange, S. Buttiglieri, M.C. Deregibus, D. Cantino, and G. Camusi. 2005. Isolation of renal progenitor cells from adult human kidney. *Am. J. Pathol.* 166:545–555.
22. Gupta, S., C. Verfaillie, D. Chmielewski, S. Kren, K. Eidman, J. Connaire, Y. Heremans, T. Lund, M. Blackstad, Y. Jiang, et al. 2006. Isolation and characterization of kidney-derived stem cells. *J. Am. Soc. Nephrol.* 17:3028–3040.
23. Challen, G.A., I. Bertoncello, J.A. Deane, S.D. Ricardo, and M.H. Little. 2006. Kidney side population reveals multilineage potential and renal functional capacity but also cellular heterogeneity. *J. Am. Soc. Nephrol.* 17:1896–1912.
24. Maeshima, A., S. Yamashita, and Y. Nojima. 2003. Identification of renal progenitor-like tubular cells that participate in the regeneration processes of the kidney. *J. Am. Soc. Nephrol.* 14:3138–3146.
25. Sagrinati, C., G.S. Netti, B. Mazzinghi, E. Lazzeri, F. Liotta, F. Frosali, E. Ronconi, C. Meini, M. Gacci, R. Squecco, et al. 2006. Isolation and characterization of multipotent progenitor cells from the Bowman's capsule of adult human kidneys. *J. Am. Soc. Nephrol.* 17:2443–2456.
26. Kollet, O., A. Dar, S. Shivtiel, A. Kalinkovich, K. Lapid, Y. Sztainberg, M. Tesio, R.M. Samstein, P. Goichberg, A. Spiegel, et al. 2006. Osteoclasts degrade endosteal components and promote mobilization of hematopoietic progenitor cells. *Nat. Med.* 12:657–664.
27. Dar, A., P. Goichberg, V. Shinder, A. Kalinkovich, O. Kollet, N. Netzer, R. Margalit, M. Zsak, A. Nagler, I. Hardan, et al. 2005. Chemokine receptor CXCR4-dependent internalization and resecretion of functional chemokine SDF-1 by bone marrow endothelial and stromal cells. *Nat. Immunol.* 6:1038–1046.
28. Fu, S., and J. Liesveld. 2000. Mobilization of hematopoietic stem cells. *Blood Rev.* 14:205–218.
29. Peled, A., I. Petit, O. Kollet, M. Magid, T. Ponomaryov, T. Byk, A. Nagler, H. Ben-Hur, A. Many, L. Shultz, et al. 1999. Dependence of human stem cell engraftment and repopulation of NOD/SCID mice on CXCR4. *Science.* 283:845–848.
30. Peled, A., O. Kollet, T. Ponomaryov, I. Petit, S. Franitza, V. Grabovsky, M.M. Slav, A. Nagler, O. Lider, R. Alon, D. Zipori, and T. Lapidot. 2000. The chemokine SDF-1 activates the integrins LFA-1, VLA-4, and VLA-5 on immature human CD34(+) cells: role in transendothelial/stromal migration and engraftment of NOD/SCID mice. *Blood.* 95:3289–3296.
31. Romagnani, P., L. Lasagni, and S. Romagnani. 2006. Peripheral blood as a source of stem cells for regenerative medicine. *Expert Opin. Biol. Ther.* 6:193–202.
32. Mohle, R., F. Bautz, S. Rafii, M.A. Moore, W. Brugger, and L. Kanz. 1998. The chemokine receptor CXCR-4 is expressed on $CD34^+$ hematopoietic progenitors and leukemic cells and mediates transendothelial migration induced by stromal cell-derived factor-1. *Blood.* 91: 4523–4530.
33. Lange, C., F. Togel, H. Ittrich, F. Clayton, C. Nolte-Ernsting, A.R. Zander, and C. Westenfelder. 2005. Administered mesenchymal stem cells enhance recovery from ischemia/reperfusion-induced acute renal failure in rats. *Kidney Int.* 68:1613–1617.
34. Broxmeyer, H.E., S. Cooper, L. Kohli, G. Hangoc, Y. Lee, C. Mantel, D.W. Clapp, and C.H. Kim. 2003. Transgenic expression of stromal cell-derived factor-1/CXC chemokine ligand 12 enhances myeloid progenitor cell survival/antiapoptosis in vitro in response to growth factor withdrawal and enhances myelopoiesis in vivo. *J. Immunol.* 170:421–429.
35. Bhakta, S., P. Hong, and O. Koc. 2006. The surface adhesion molecule CXCR4 stimulates mesenchymal stem cell migration to stromal cell-derived factor-1 in vitro but does not decrease apoptosis under serum deprivation. *Cardiovasc. Revasc. Med.* 7:19–24.
36. Kunduzova, O.R., G. Escourrou, F. De La Farge, R. Salvayre, M.H. Seguelas, N. Leducq, F. Bono, J.M. Herbert, and A. Parini. 2004. Involvement of peripheral benzodiazepine receptor in the oxidative stress, death-signaling pathways, and renal injury induced by ischemia-reperfusion. *J. Am. Soc. Nephrol.* 15:2152–2160.
37. Sachse, A., and G. Wolf. 2007. Angiotensin II-induced reactive oxygen species and the kidney. *J. Am. Soc. Nephrol.* 18:2439–2446.
38. Zager, R.A. 1992. Combined mannitol and deferoxamine therapy for myohemoglobinuric renal injury and oxidant tubular stress. Mechanistic and therapeutic implications. *J. Clin. Invest.* 90:711–719.
39. Mazo, I.B., E.J. Quackenbush, J.B. Lowe, and U.H. von Andrian. 2002. Total body irradiation causes profound changes in endothelial traffic molecules for hematopoietic progenitor cell recruitment to bone marrow. *Blood.* 99:4182–4191.
40. Romagnani, P., L. Lasagni, F. Annunziato, M. Serio, and S. Romagnani. 2004. CXC chemokines: the regulatory link between inflammation and angiogenesis. *Trends Immunol.* 25:201–209.
41. Nowak, G., P.M. Price, and R.G. Schnellmann. 2003. Lack of a functional $p21^{WAF1/CIP1}$ gene accelerates caspase-independent apoptosis induced by cisplatin in renal cells. *Am. J. Physiol. Renal Physiol.* 285:F440–F450.
42. Romagnani, P., F. Annunziato, F. Liotta, E. Lazzeri, B. Mazzinghi, F. Frosali, L. Cosmi, L. Maggi, L. Lasagni, S. Scheffold, et al. 2005. CD14+CD34low cells with stem cell phenotypic and functional features are the major source of circulating endothelial progenitors. *Circ. Res.* 97:314–322.
43. Lasagni, L., M. Francalanci, F. Annunziato, E. Lazzeri, S. Giannini, L. Cosmi, C. Sagrinati, B. Mazzinghi, C. Orlando, E. Maggi, et al. 2003. An alternatively spliced variant of CXCR3 mediates the inhibition of endothelial cell growth induced by IP-10, Mig, and I-TAC, and acts as functional receptor for platelet factor 4. *J. Exp. Med.* 197:1537–1549.
44. Munson, P.J., and D. Rodbard. 1980. LIGAND: a versatile computerized approach for characterization of ligand-binding systems. *Anal. Biochem.* 107:220–239.
45. Romagnani, P., F. Annunziato, L. Lasagni, E. Lazzeri, C. Beltrame, M. Francalanci, M. Uguccioni, G. Galli, L. Cosmi, L. Maurenzig, et al. 2001. Cell cycle-dependent expression of CXC chemokine receptor 3 by endothelial cells mediates angiostatic activity. *J. Clin. Invest.* 107:53–63.